Design and Control of a Reclining Chair with Soft Pneumatic Cushions

Design and Control of a Reclining Chair with Soft Pneumatic Cushions

Marco Bellusci[1], Carlo Ferraresi[1], Giovanni Gerardo Muscolo[2]

[1] Department of Mechanical and Aerospace Engineering, Politecnico di Torino, Italy
[2] Department of Computer Science, University of Verona, Italy
giovannigerardo.muscolo@univr.it

Abstract. The object of this work is the control of a reclining chair with active cushions used to optimize the interaction of the human with the chair and to avoid the formation of sores on the skin. The cushion system, already presented in other works, consists of air-cell actuators distributed according to the risk that pressure ulcers on the skin can be generated in certain areas. In this work, four cushions are designed and controlled for four parts of the human body: 1) head; 2) back; 3) buttocks; 4) heels. Cushions are used to design a reclining chair that can be moved between two configuration limits: a) chair; b) bed. The four cushions can provide real-time pressure mapping with closed-loop control, which allows to identify critical points on the body surface where pressure ulcers could form. The control systems for the single air-cell and for all cushions are designed and simulated using the software MATLAB/Simulink, presenting very interesting results.

Keywords: Pressure Injury, Automated Seat Cushion, Reclining Chair, Bubble Actuators, Soft Actuators, Pneumatic Actuators, Pressure Ulcers.

1 Introduction

Once called bedsores, Pressure Injuries (PIs) are localized damage to the skin and the underlying soft tissue. They are usually localized under bony prominences (like the tailbone and heels) [1]. The formation of PIs depends both on direct and indirect factors [2]. The most important cause of ulceration is a prolonged pressure between the bony prominence and the external surface that occluding the capillaries [3]. The formation of a PI is directly proportional to the pressure applied and the period for which it is applied: even a low pressure can generate a PI if applied for a long period [4]. Concomitant with pressure, shear is always present. Blood vessels are stretched and torn by this shearing, favoring the formation of PIs. Some other causes of PIs that must be considered are moisture, friction, the position of the patient, immobility, aging, diabetes, and neurological factors [3]. Pressure ulcers have been increasing in the last years due to an incremented average age of the population and this means that also the costs related to this problem are growing [5]. The National Pressure Injury Advisory Panel (NPIAP) classified the PIs in four major stages [1]. In particular, the average hospital treatment cost of stage 4 pressure ulcers is very high, around $129,124 for PIs acquired during

one admission at the hospital [6]. Different studies have shown how adopting a prevention protocol in long-term care is cost reducing with respect to treating PIs once they have developed [7, 8]. Different treatments for PIs are available in the literature. The first simple strategy is repositioning. Doctors suggest repositioning the patient every 2 hours but there are no robust evidence on the best repositioning frequency and position [9]. Specific support surfaces like mattresses, beds, cushions, and overlays have been designed in order to reduce pressure magnitude and minimize shear. They can be classified as constant low-pressure (CLP) devices, which conform to body shape, or alternating pressure (AP) devices, where the pressure is mechanically varied [10]. CLP supports have been proven to be preferable with respect to standard foam hospital mattresses. Several alternatives have been studied like high-specification foam, bead-filled and water filled. However, no significant difference has been noticed between the different possible materials for a CLP support [10]. Using AP mattresses can delay 11 days the formation of a PI and have an 80% probability of being cost saving [11]. However, the AP algorithms consider only the body weight, neglecting other important parameters like body prominences, asymmetry, and bad posture [12]. Another drawback is the bottom out problem: the original shape and property of the air-filled compartments can be altered due to an excessive load or other external disturbances (aging, wear, weak maintenance) [13]. AP devices have a passive control mechanism where air-cells are repeatedly inflated or deflated regardless of the pressed regions and pressure level. To solve this problem, active support surfaces were introduced. These dynamic solutions are still characterized by air-filled compartments, but the air-cells are inflated and deflated based on the measured pressure above them [14, 15]. The reference pressure is compared with the measured one and the result is used to proportionally deflate or inflate the air-cells. It has been proven that this approach not only involves a redistribution of body weight but also better reperfusion and good comfort [16]. In [17], a first design of the air-cell actuators of one seat cushion has been presented and controlled. In this work, we optimized the control of the air-cell actuators and proposed a novel design for a reclined chair constituted of four cushions: Head, Back, Seat, Heel (see Fig. 1).

2 Design of the Automated Reclining Chair

Figure 1 shows the reclining chair with four cushions (head, back, seat, heel) connected through two joints and each of them can be controlled by an external input. The overall dimensions of the cushions are designed considering the sitting position of the standard man (age 30, weight 70 kg, height 1.72 m) [18]. The reclining chair has two rotary joints that can rotate of 90° allowing to assume different shapes between two limit configurations: a) chair, in which both the joints are at rest and the reclining chair has the same shape as shown in Fig. 1; b) bed, in which both joints are turned 90°, respect to Fig. 1, and the four cushions are aligned composing a sort of bed. The cushions composing the reclining chair have been designed considering the areas more at risk of developing the PIs when lying in a bed, in particular: back of head and ears, shoulder and back, elbows, lower back and buttocks, greater trochanter, heel [19]. An innovation

introduced in the cushions of this work and presented in [17], respect to the proposed in literature [14-16], is that the air-cells are inflated or deflated in group making the system quicker to respond to the stimulus but also more accurate since these groups are correlated to the different areas, classified according to the risk of developing PIs. While sitting, the body weight mainly concentrates in the buttocks and the thigh regions, but it largely depends on the adopted sitting posture and on the type of chair [14].

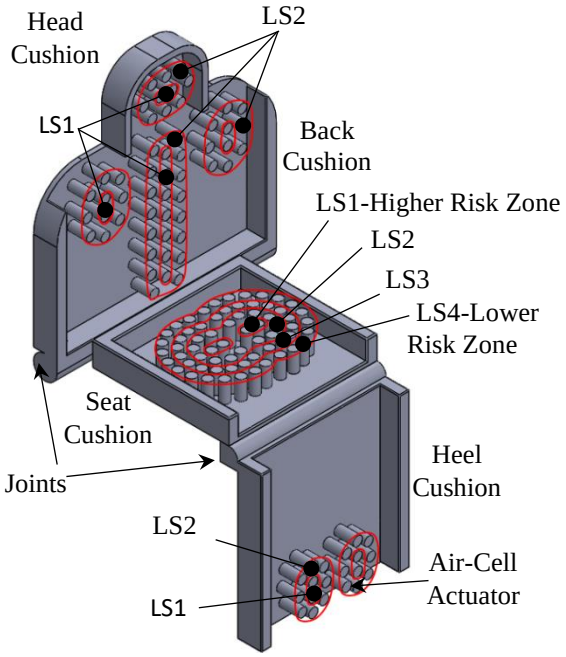

Fig. 1. 3D model of the reclining chair with four cushions: Head, Back, Seat, Heel.

Different studies using dynamic pressure mapping have proven that the highest-pressure values are below the Ischial Tuberosities (ITs) and the coccyx [16, 17]. Other studies have also confirmed that these regions are the more interested in shear and deformation effects [17, 18]. Starting from the buttock region more at risk, four Level Surfaces (LSs) have been designed, as shown in Fig. 1. The LSs are numbered starting from the internal one. The seat cushion, presented in [17], is composed of 66 air-cells distributed on the cushion in the following way: 4 cylinders inside the LS1; 14 cylinders inside the LS2; 22 cylinders inside the LS3; 26 cylinders inside the LS4 [17]. The pressure on the head, back and heel cushions goes from almost zero in the chair configuration to bigger values while the bed configuration is being reached. Two LSs have been introduced in the head, back and heel cushions. Each LS is constituted by a defined number of air-cells, which are activated and deactivated together. The two LSs are related to the higher and lower risk zones of pressure ulcers generation. The LS1 is delimited by the internal Level Curve (LC1) and the LS2 is delimited by the LC1 and the external Level Curve (LC2). In the head cushion, the air-cells of LS1 are two, while there are eight air-cells inside the LS2. In the back cushion, the air-cells of LS1 are

eleven and they are disposed along the shoulder and the back, considering 500 mm the average distance between the arms. Thirty-two air-cells form the LS2. In the heel cushion, four air-cells form the LS1 and are disposed considering the average distance between the two legs equal to 150 mm. The LS2 instead contains sixteen air-cells.

3 Analytical Modelling of the Air-Cells

The air-cells have been optimized with a Finite Element (FE) analysis in [17]. They have a cylindrical shape with an outer diameter of 30 mm, a height of 65 mm and a thickness of 1.2 mm. Moreover, silicon rubber is selected as the material for the cylinders [20, 21]. If the change in the contact area ($A_{contact}$) between the load (F_{ext}) and the air-cell is neglectable, the interface pressure (p) is simply obtained by the following relation:

$$p = \frac{F_{ext}}{A_{contact}} \tag{1}$$

In our system, the pressure inside each level surface must be adjusted proportionally to a given command. The regulation is carried out by means of two two-port digital valves controlled in Pulse Width Modulation (PWM) (see Fig. 2a). A first valve (supply valve) connects the LS to the air supply, the second (exhaust valve) connects the LS to the ambiance. The entire seat cushion, therefore, requires only eight very inexpensive valves to be controlled, reducing significantly the cost. More details on the general control system of an air-cell can be found in [17]. The air-cells can be considered such as an elastic tank receiving an air flow $G(t)$ from the digital valves and an external force from the mass of the person using the cushion. The temperature T is assumed constant while the volume $V(t)$, the pressure $p(t)$, and the density ρ are free to change. Considering the transformation as polytrophic, the pneumatic continuity equation of the air-cell is

$$\frac{dp}{dt} = \frac{GnRT_i}{V}\left(\frac{p}{p_i}\right)^{\frac{1-n}{n}} - \frac{pn}{V}\frac{dV}{dt} \tag{2}$$

4 Control System Architecture

A closed-loop control system has been used to control the internal pressure of the air-cell. Therefore, the air-cell is the plant of our system while the two valves are the actuators (as shown in Fig. 2b). A manual switch allows to quickly change the pressure reference input from a step signal to a trapezoidal signal, or vice-versa. The tracking error e(t) enters the controller (red block), which generates the PWM commands to the digital valves. The computed airflows reach the plant (green block) composed of two blocks. In the air-cell pressure block the instantaneous pressure p(t) of the air-cell is calculated integrating equation 2). In the air-cell block, the volume V(t) of the air-cell, its derivative dV/dt, and the height h(t) are computed. In particular, the volume V(t)

and the displacement z(t) were obtained through an interpolation of data measured with FE analysis [17].

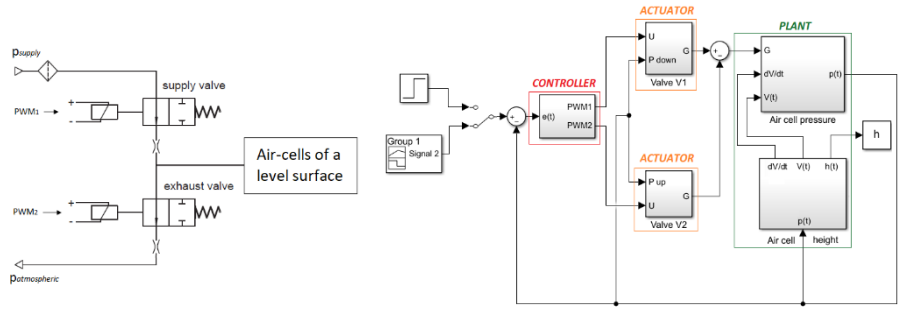

a) b)

Fig. 2. Supply and exhaust valve connected to a level surface (a); Simulink feedback control system of the single air-cell (b).

Each cushion is studied considering a certain force distribution over it. In the seat cushion a 9N load on the LS1, 7N on the LS2, 5N on the LS3, and 3N on the LS4 are applied [17]. Each LS block is equal to the system of a single air-cell of Fig. 2b, but with different input data for volume, pressure and displacement, derived from the different FE analyses [17]. The total volume is set proportionally to the number of actuators inside the specific LS. Two different approaches have been studied. In the first one, the LSs are controlled in series; in the second one, the LSs are controlled in parallel. In the series configuration, the control of a LS starts only when the previous LS has reached the steady-state condition; in the parallel configuration the control of all the level surfaces starts simultaneously. This method is used to observe the inflation and the deflation of the four LSs in the seat cushion [17].

5 Results and Discussions

For the reference signal of the single air cell, two kinds of input have been used, a step signal and a trapezoidal signal. The results have been obtained implementing the control architecture of Fig. 2 and are shown in Fig. 3. The pressure p(t) tracks well the pressure set. From the step response, it can be noticed that the system is critically damped and has a rise time of 0.5s. Figure 4 shows the simulation performed for the head, back and heel cushions. The simulations are performed using a supply pressure of 131.3 kPa for the LS1 and a supply pressure of 301.3 kPa for the LS2. Loads of 7N and 5N are applied on the air-cells of LS1 and LS2 respectively. The control system of the head cushion is faster than the other two because of the smaller number of air-cells to inflate/deflate but all the three cushions have a good ability in tracking the input. It is possible to note that in each cushion the control of LS1 is faster due to the smaller number of air-cells.

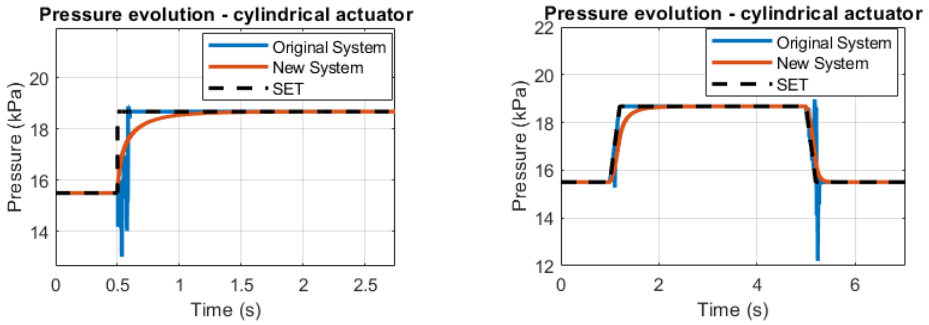

Fig. 3. System output with a step input (on the left) and a trapezoidal input (on the right) for the single air-cell.

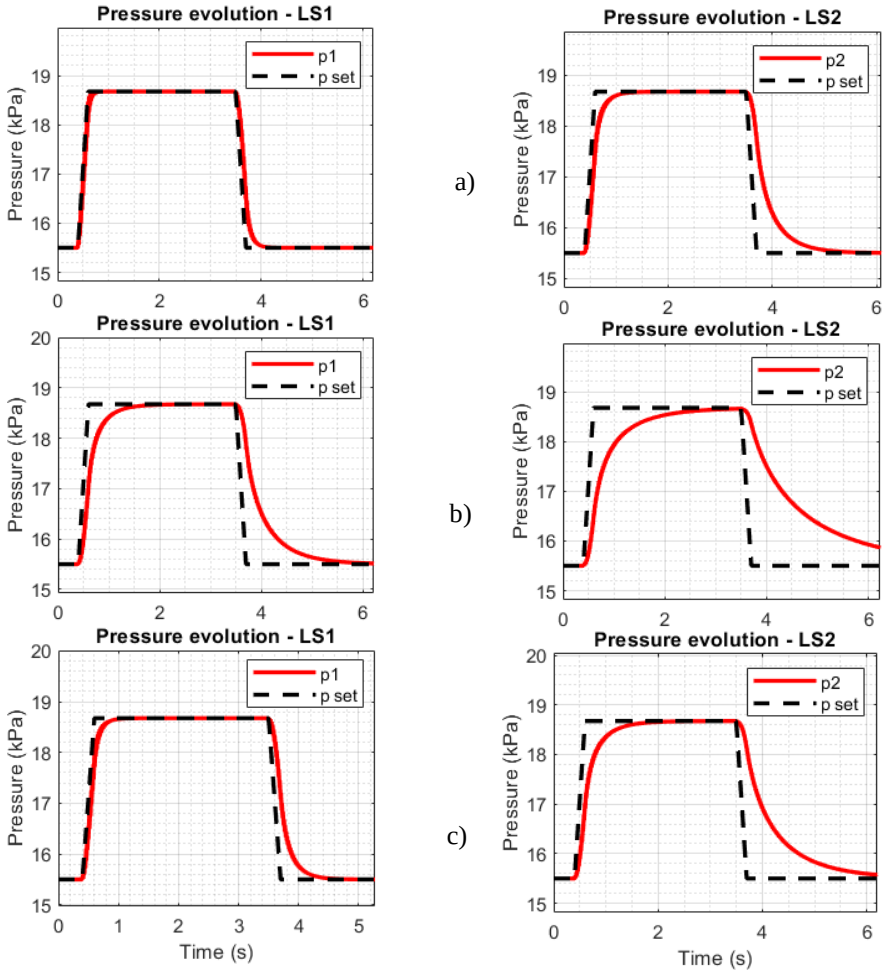

Fig. 4. Pressures evolution in head (a), back (b), and heel (c) cushions.

6 Conclusion

The objective of this work was the development of a reclining chair composed by automated cushions for pressure ulcer prevention. A previous work [17] was focused on improving the control system of a single air-cell that composes the contact surface of the seat cushion. In this work, the development of the control system for the four different cushions composing a complete reclining chair is presented. Head, back and heel cushions, together with the previously developed buttocks cushion, compose the reclining chair, which can be moved between two limits configuration: a) chair and b) bed. The three new cushions are designed such that, again, particular attention was given to the more at-risk area of the body (back of head and ears, shoulder and back, elbows, lower back and buttocks, greater trochanter, heel). Therefore, each cushion has its own number of air-cells and its own distribution of them. Only two-level surfaces were used since they have to respond to lower load levels with respect to the buttocks cushion. Even for these cushions, the results of simulations highlighted a good behavior of the developed control system, which is able to reach with good dynamic performance the optimal pressure with any external loads and initial pressure conditions.

References

1. Edsberg, L. E., Black, J. M., Goldberg, M., McNichol, L., Moore, L., & Sieggreen, M. (2016). Revised National Pressure Ulcer Advisory Panel pressure injury staging system: revised pressure injury staging system. Journal of Wound, Ostomy, and Continence Nursing, 43(6), 585.
2. Bhattacharya, S., & Mishra, R. K. (2015). Pressure ulcers: current understanding and newer modalities of treatment. Indian Journal of Plastic Surgery, 48(01), 004-016.
3. Agrawal, K., & Chauhan, N. (2012). Pressure ulcers: Back to the basics. Indian Journal of Plastic Surgery, 45(02), 244-254.
4. Bernabei, R., Manes-Gravina, E., & Mammarella, F. (2011). Epidemiologia delle piaghe da decubito. G Gerontol, 59, 237-43.
5. Jaul, E. (2010). Assessment and management of pressure ulcers in the elderly. Drugs & aging, 27(4), 311-325.
6. Brem, H., Maggi, J., Nierman, D., Rolnitzky, L., Bell, D., Rennert, R., ... & Vladeck, B. (2010). High cost of stage IV pressure ulcers. The American Journal of Surgery, 200(4), 473-477.
7. Xakellis, J. G., Frantz, R. A., Lewis, A., & Harvey, P. (1998). Cost-effectiveness of an intensive pressure ulcer prevention protocol in long-term care. Advances in wound care: the journal for prevention and healing, 11(1), 22-29.
8. Pham, B., Stern, A., Padula, W. V., Mishra, M. K., Makic, M. B. F., & Sullivan, P. W. (2012). Improving the quality of pressure ulcer care with prevention: A cost-effectiveness analysis. Medical care, 50(2), 188-190.
9. Gillespie, B. M., Chaboyer, W. P., McInnes, E., Kent, B., Whitty, J. A., & Thalib, L. (2014). Repositioning for pressure ulcer prevention in adults. Cochrane Database of Systematic Reviews, (4).
10. Mervis, J. S., & Phillips, T. J. (2019). Pressure ulcers: prevention and management. Journal of the American Academy of Dermatology, 81(4), 893-902.

11. Iglesias, C., Nixon, J., Cranny, G., Nelson, E. A., Hawkins, K., Phillips, A., ... & Cullum, N. (2006). Pressure relieving support surfaces (PRESSURE) trial: cost effectiveness analysis. Bmj, 332(7555), 1416.
12. Saegusa, M., Noguchi, H., Nakagami, G., Mori, T., & Sanada, H. (2018). Evaluation of comfort associated with the use of a robotic mattress with an interface pressure mapping system and automatic inner air-cell pressure adjustment function in healthy volunteers. Journal of tissue viability, 27(3), 146-152.
13. Hollington, J., Hillman, S. J., Torres-Sánchez, C., Boeckx, J., & Crossan, N. (2014). ISO 16840-2: 2007 load deflection and hysteresis measurements for a sample of wheelchair seating cushions. Medical engineering & physics, 36(4), 509-515.
14. Carrigan, W., Nuthi, P., Pande, C., Nothnagle, C. P., & Wijesundara, M. B. (2017). A Pressure modulating sensorized soft actuator array for pressure ulcer prevention. In ASME 2017 International Design Engineering Technical Conferences and Computers and Information in Engineering Conference. American Society of Mechanical Engineers Digital Collection.
15. Wijesundara, M., & Cooper, R. (2016). Automated Seat Cushion for Pressure Ulcer Prevention Using Real-Time Mapping, Offloading, and Redistribution of Interface Pressure. University of Texas at Arlington Arlington United States.
16. Carrigan, W., Nuthi, P., Pande, C., Wijesundara, M. B., Chung, C. S., Grindle, G. G., ... & Cooper, R. A. (2019). Design and operation verification of an automated pressure mapping and modulating seat cushion for pressure ulcer prevention. Medical engineering & physics, 69, 17-27.
17. Mannella D, Bellusci M, Graziani F, Ferraresi C, Muscolo G G. “Modelling, design and control of a new seat-cushion for pressure ulcers prevention”. Proceedings of the Institution of Mechanical Engineers, Part H: Journal of Engineering in Medicine. January 2022. doi:10.1177/09544119211068908
18. Maiorino A and Muscolo GG (2020). “Biped Robots With Compliant Joints for Walking and Running Performance Growing”. Front. Mech. Eng. 6:11. doi: 10.3389/fmech.2020.00011
19. Sonenblum, S. E., Sprigle, S. H., Cathcart, J. M., & Winder, R. J. (2015). 3D anatomy and deformation of the seated buttocks. Journal of tissue viability, 24(2), 51-61.
20. G.G. Muscolo and M. Fontana, “A novel linear pneumatic actuator with tunable-compliance constraint”, International Journal of Mechanics and Control, ISSN: 1590-8844, Vol. 21, No. 02, 2020, pp. 73-85.
21. Bottero, S.; Muscolo, G.G.; Ferraresi, C. “A New Soft RCC Device with Pneumatic Regulation”. Robotics 2020, 9, 98. https://doi.org/10.3390/robotics9040098